A single-layer, planar, optofluidic switch powered by acoustically driven, oscillating microbubbles

Po-Hsun Huang, Michael Ian Lapsley, Daniel Ahmed, Yuchao Chen, Lin Wang et al.

Citation: Appl. Phys. Lett. **101**, 141101 (2012); doi: 10.1063/1.4742864
View online: http://dx.doi.org/10.1063/1.4742864
View Table of Contents: http://apl.aip.org/resource/1/APPLAB/v101/i14
Published by the American Institute of Physics.

A single-layer, planar, optofluidic switch powered by acoustically driven, oscillating microbubbles

Po-Hsun Huang,[1] Michael Ian Lapsley,[1] Daniel Ahmed,[1] Yuchao Chen,[1] Lin Wang,[2] and Tony Jun Huang[1,a)]
[1]*Department of Engineering Science and Mechanics, The Pennsylvania State University, University Park, Pennsylvania 16802, USA*
[2]*Ascent Bio-Nano Technologies Inc., State College, Pennsylvania 16801, USA*

(Received 30 May 2012; accepted 20 July 2012; published online 1 October 2012)

Merging acoustofluidic mixing with optofluidic integration, we have demonstrated a single-layer, planar, optofluidic switch that is driven by acoustically excited oscillating microbubbles. The device was found to have a switching speed of 5 Hz, an insertion loss of 6.02 dB, and an extinction ratio of 28.48 dB. With its simplicity, low fluid consumption, and compatibility with other microfluidic devices, our design could lead to a line of inexpensive, yet effective optical switches for many lab-on-a-chip applications. © *2012 American Institute of Physics*. [http://dx.doi.org/10.1063/1.4742864]

Optofluidics, the fusion of optics and microfluidics, exploits the unique properties of liquids (e.g., excellent reconfigurability, laminar flow, diffusion) and provides excellent opportunities to manipulate light in an unprecedented manner.[1–8] In recent years, optofluidic techniques have led to the development of optical prisms,[9] lenses,[5,10–12] light sources,[13] interferometers,[14,15] filters,[16] optical tweezers,[17] and switches.[18] In particular, significant effort has been devoted to the development of low-cost, disposable optofluidic switches for "low-end" optical switching and lab-on-a-chip applications. Most of these optofluidic switches operate based on flow rate moderation[19–22] or pneumatic pressure.[23,24] The optofluidic switches based on flow rate moderation tend to consume large amounts of liquid to acquire high switching rates, which make the device bulky and difficult to maintain. The optofluidic switches based on pneumatic pressure require many bulky external components, such as microsolenoid valves, to control the fluid or air for switching, and these switches are typically prepared using multi-layer fabrication processes, which increase cost and complicate the fabrication process. Therefore, it is desirable to develop alternate optofluidic switches which are affordable, easy to fabricate, and operate with less dependence on high flow rates and expensive external equipment.

In this work, we introduce a single-layer, planar, optofluidic switch based on a tunable reflective interface, in which an acoustically driven, bubble-based, fast micromixer was used to mix the input fluids, thus, altering the refractive index of the fluid in the channel and switching the reflectivity of the channel sidewall. The speed of our acoustically driven, optofluidic switch is dependent on the mixing time rather than the flow rate of the fluid, thus, significantly reducing the volume of fluid needed for switching. In addition, compared to existing optofluidic switches, our device has a much simpler fabrication process (single-layer device vs. multi-layer device) and does not require expensive external equipment.

Figure 1 schematically shows the design and working principle of our acoustically driven optofluidic switch. This device was fabricated using standard soft lithography. It included a main microchannel with two inlets and one outlet, predesigned cavities on the sidewall of the main microchannel to trap bubbles for mixing, two side channels for inserting and aligning the optical fibers, and two air-polydimethysiloxane (PDMS) lenses (radii of 164 μm) to collimate the light.[25] The microchannel was 120 μm wide, the optical slots were 125 μm wide, and all features were 130 μm tall. The surface of the PDMS device was treated with oxygen plasma and bonded onto a glass slide. A piezoelectric transducer (model no. 273-073, RadioShack), used to oscillate the sidewall-trapped microbubbles,[26–28] was bonded using epoxy (Devcon 2 Ton Epoxy) onto the same glass slide, and the piezoelectric transducer was driven by a function generator (Hewlett Packard 8166A). The experiment was monitored visually on a Nikon TE-2000U optical microscope. Two fluids were injected at the fluid inputs using 1 ml syringes pumped by two separate syringe pumps. One syringe was filled with de-ionized (DI) water (refractive index: $n_1 = 1.333$) and the other syringe was filled with a 4 M solution of $CaCl_2$ ($n_2 = 1.423$). The input optical fiber was a single-mode fiber with a numerical aperture of 0.14, and the output fiber was a multimode fiber with a core size of 105 μm and a numerical aperture of 0.22. A fiber-coupled laser (Blue Sky, 488 nm, 20 mW) provided light to the input fiber, while a photomultiplier tube (PMT) was connected to the output fiber. The signal from the PMT was recorded on a digitizing Tektronix oscilloscope. The fibers were aligned at the side of the channel in contact with the water flow at an angle, such that when water fills the channel, the light will experience total internal reflection (TIR). The critical angle for TIR at an interface between PDMS ($n_4 = 1.414$) and DI water ($n_1 = 1.333$) is 70.5°. To ensure TIR, the angle between the two fibers was 72.0°, and the insertion loss for this system was 6.02 dB.

When the piezoelectric transducer was turned off, the reflective interface was formed by PDMS and pure DI water, thus, almost the entire incident beam was reflected and recorded by the output optical fiber as shown schematically in Fig. 1(a). Figures 2(a) and 2(b) show optical

a)Author to whom correspondence should be addressed. Electronic mail: junhuang@psu.edu.

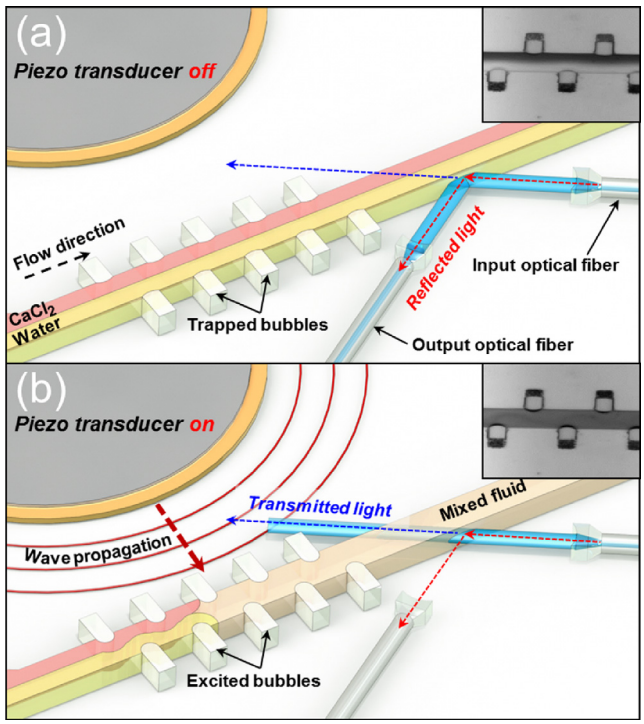

FIG. 1. A schematic showing the design and working principle of the oscillating bubble-based optofluidic switch. (a) The device under acoustic excitation; (b) the device without acoustic excitation.

microscope images of the device in this state and verify that no acoustic streaming was present and that the majority of the incident laser beam was reflected and recorded by the output fiber. In this case, we define that the device is in the "on" mode. When the piezoelectric transducer was turned on, the device was in the "off" mode: the trapped bubbles were acoustically oscillated, mixing the two fluids; as a result, the refractive index of the mixed solution (n_3) would be closer to n_4 and reduce the reflection [Fig. 1(b)]. The optical images in Figs. 2(c) and 2(d) indicate acoustic streaming is present and the majority of the light is transmitted. In all the experiments, the driving voltage and frequency were fixed at 18 VPP and 108 kHz, respectively.

The flow rate of water (Q_1) always remained two times larger than that of the $CaCl_2$ solution (Q_2), in order to compensate for the viscosity-induced interface shift[29] and place the interface in the center of the channel. When the flow rate was such that complete mixing was achieved during the "off" state, the refractive index of the fluid would be the average of n_1 and n_2; thus, the refractive index of the fully mixed solution would be $n_3 = 1.378$. Based on the analysis in our previous work,[25] this refractive index would cause an attenuation of approximately -15 dB in the reflection. Thus, most of the incident laser beam will pass through the microchannel instead of reflecting at the interface, and only small amount of the beam will be reflected and recorded [Fig. 2(d)].

We further characterized the switching response of the device by measuring the dynamics of the change in reflectivity recorded by the PMT. Figure 3 shows the normalized waveforms from the PMT when the device was operated under different total flow rates ($Q_T = Q_1 + Q_2$). In Fig. 3, two standard references (blue and red curves) are shown with the signals, and the signals were normalized to these references. The standard reference for maximum reflection (Fig. 3, blue curve) was produced by recording data while the channel was filled only with DI water (attenuation of 0 dB). The standard for minimum reflection (Fig. 3, red curve) was produced by recording data while the channel was filled only with a 4 M solution of $CaCl_2$ (attenuation of -30 dB).[25] Figure 3(a) is an example of a signal recorded at a relatively low flow rate ($Q_T = 7.5$ μl/min). In this case, the reflectivity at the "on" mode (i.e., the high side of the signal) is lower than the standard reference for maximum reflection (Fig. 3, blue curve). The decreased reflectivity was attributed to premixing caused by diffusion. As Q_T was increased, the premixing was reduced and the reflectivity at the "on" mode gets closer to the standard reference for maximum reflection [Fig. 3(b)]. Once Q_T was high enough to avoid premixing, the reflectivity at the "on" mode almost exactly matches with the standard reference for maximum reflection [Fig. 3(c)].

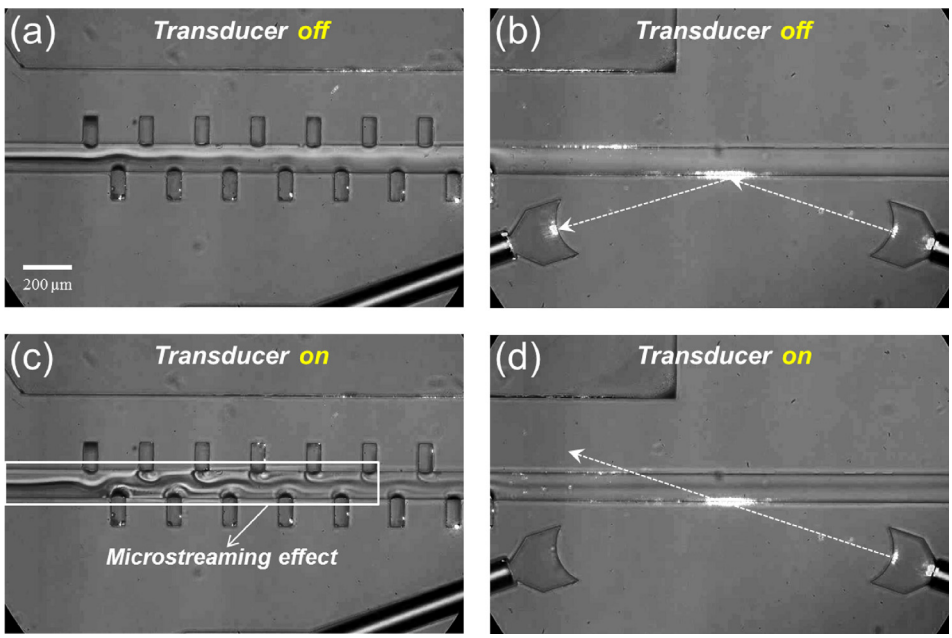

FIG. 2. Experimental images of the optofluidic switch. (a) and (b) The device without acoustic excitation. (c) and (d) The device under acoustic excitation where microstreaming is observed. The dotted arrow represents the light path.

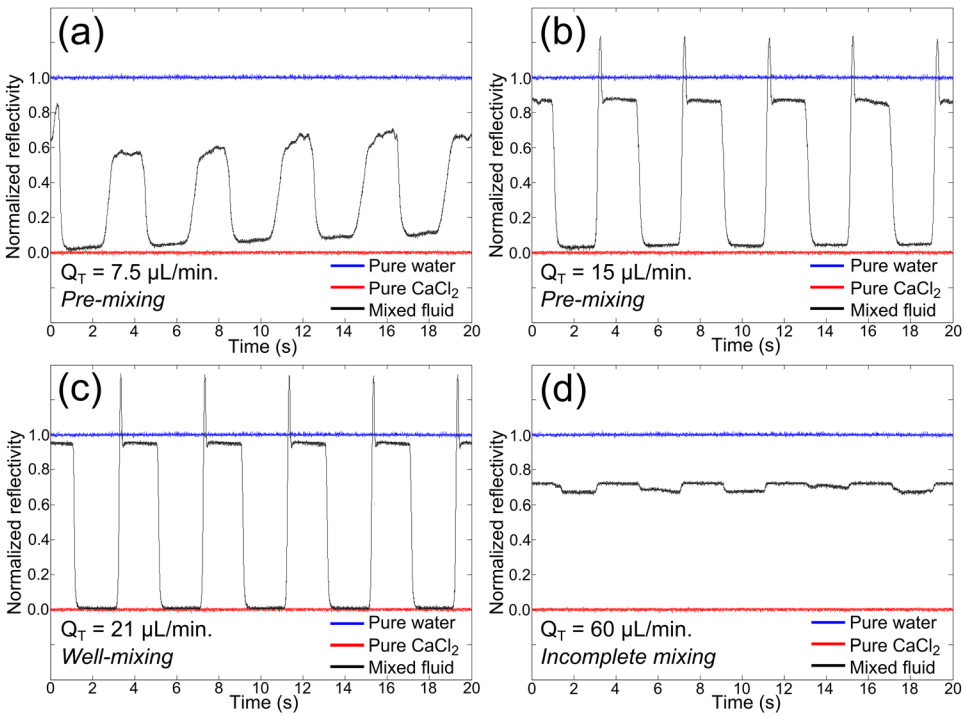

FIG. 3. The normalized signal waveforms under different total flow rates ($Q_T = Q_1 + Q_2$). (a) $Q_T = 7.5$ μl/min; (b) $Q_T = 15$ μl/min; (c) $Q_T = 21$ μl/min; (d) $Q_T = 60$ μl/min.

If Q_T was further increased, the reflectivity signals at the "on" and "off" modes deviate significantly from the two reference standards [Fig. 3(d)]. The deviation of the reflectivity signals during the "off" mode from the standard reference for the minimum reflection was attributed to incomplete mixing due to the high flow suppressing the microstreaming caused by the oscillation of the bubble. The deviation of the reflectivity signals during the "on" mode from the standard reference for the maximum reflection can be explained by the instability of sidewall-trapped bubbles at high Q_T. At high Q_T the bubbles tend to expand and partially protrude into the microchannel, making the fluid path curved and such a curved path causes mixing.[30] As a result, we can also observe premixing at very high Q_T. The instability of sidewall-trapped bubbles at high Q_T could be improved by stabilizing the surface of the bubble. Essentially, our device is not designed for operating at high Q_T because at high flow rates, large amount of fluids would be wasted. Nevertheless, we tested our device at different Q_T in order to define its limitations and working range. It should also be noted that there were overshoot peaks observed at the moment of switching from the "off" mode to the "on" mode [Figs. 3(b) and 3(c)]. We suspect that instabilities in the mixed fluid right after the piezoelectric transducer is turned off cause a gradient of concentration in the vertical direction. Such a gradient could cause some focusing or collimation of the light which would otherwise continuously expand in the vertical direction. Such focusing or collimation could cause the reflectivity to exceed the standard reference for maximum reflection, as seen in our data. This phenomenon affected the performance of the switch, thus, we introduced the parameter of settling time to quantify this effect.

Next, we performed a set of experiments to quantify the dynamic response of our device. Figure 4 displays several characteristics of interest (rising time, falling time, and extinction ratio) as a function of Q_T. The extinction ratio,[20] a

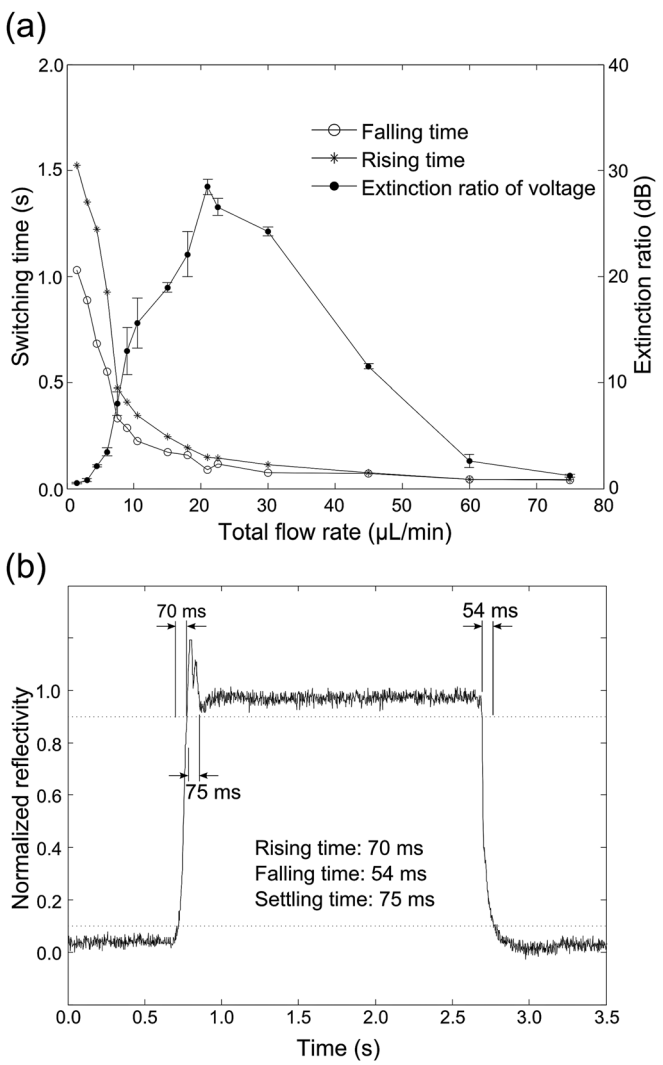

FIG. 4. (a) Switching performance in response to total flow rate. (b) Analysis of the dynamic response of the device.

typical parameter to characterize the efficiency of a switch, is defined as the ratio between the output intensity when the switch is on and that when the switch is off. As Q_T of the mixed solution increased, the rising and falling time decreased, improving the switching speed; however, the extinction ratio was only acceptable over a range of flow rates. Based on Fig. 4(a), we identified the acceptable working range of Q_T to be between 15 and 30 μl/min for our device. When the Q_T was lower than 15 μl/min, the switch suffered from premixing as observed in Fig. 3(a), causing a low extinction ratio. Similarly, when Q_T exceeded 30 μl/min, the switch suffered due to incomplete mixing [Fig. 3(d)]. The maximum extinction ratio of 28.48 dB was observed at $Q_T = 21$ μl/min, and the dynamic response at this flow rate yielded a switching time (sum of rising, falling, and settling time) of $\sim$200 ms, which corresponds to a switching frequency of $\sim$5 Hz [Fig. 4(b)]. The switching time could be improved by fine-tuning the system to remove the effects which cause overshoot and large settling times. The extinction ratio could be improved by increasing the concentration of $CaCl_2$ solution to make the mixed fluid with higher refractive index, meaning that a smaller amount of incident laser beam will be reflected in the "off" mode. With our device, the frequency at which the signal from the function generator is turned on and off (0.25 Hz as seen in Fig. 3) could be adjusted. By taking advantage of the ability to modulate this frequency, any digital electrical signal (in series) could be applied to this device, and thus any digital optical signal (in series) could be generated.

In conclusion, we fabricated and tested an optofluidic switch that operates by oscillating microbubbles to produce the microstreaming effects to mix two fluids, thus, altering the refractive index of a PDMS/fluid interface. An insertion loss of 6.02 dB, extinction ratio of 28.48 dB, and switching speed of 200 ms (5 Hz) were achieved for this device. Our device offers advantages such as simple operation and high extinction ratios. In addition, this system reduces the need for extremely high flow rates to achieve fast switching, and could be integrated into in-plane optofluidic modules and microfluidic devices with precise alignment for reconfigurable miniaturized optical systems and lab-on-a-chip applications.

This work was supported by the National Institutes of Health (NIH) Director's New Innovation Award (1DP2OD007209-01), National Science Foundation (NSF), and the Penn State Center for Nanoscale Science (MRSEC). Components of this work were conducted at the Penn State node of the NSF-funded National Nanotechnology Infrastructure Network.

[1]D. Psaltis, S. R. Quake, and C. H. Yang, Nature **442**, 381 (2006).
[2]C. Monat, P. Domachuk, and B. J. Eggleton, Nat. Photonics **1**, 106 (2007).
[3]S. K. Y. Tang, C. A. Stan, and G. M. Whitesides, Lab Chip **8**, 395 (2008).
[4]X. Mao, J. R. Waldeisen, B. K. Juluri, and T. J. Huang, Lab Chip **7**, 1303 (2007).
[5]S. K. Y. Tang, R. Derda, Q. Quan, M. Loncar, and G. M. Whitesides, Opt. Express **19**, 2204 (2011).
[6]C. Escobedo, A. G. Brolo, R. Gordon, and D. Sinton, Nano Lett. **12**, 1592 (2012).
[7]A. J. Chung and D. Erickson, Opt. Express **19**, 8602 (2011).
[8]X. Mao, A. A. Nawaz, S. C. S. Lin, M. I. Lapsley, Y. Zhao, J. P. McCoy, W. S. El-Deiry, and T. J. Huang, Biomicrofluidics **6**, 024113 (2012).
[9]S. Xiong, A. Q. Liu, L. K. Chin, and Y. Yang, Lab Chip **11**, 1864 (2011).
[10]Y. C. Seow, A. Q. Liu, L. K. Chin, X. C. Li, H. J. Huang, T. H. Cheng, and X. Q. Zhou, Appl. Phys. Lett. **93**, 084101 (2008).
[11]X. Mao, Z. I. Stratton, A. A. Nawaz, S. C. S. Lin, and T. J. Huang, Biomicrofluidics **4**, 043007 (2010).
[12]X. Mao, S. C. S. Lin, M. I. Lapsley, J. Shi, B. K. Juluri, and T. J. Huang, Lab Chip **9**, 2050 (2009).
[13]W. Z. Song, A. E. Vasdekis, Z. Y. Li, and D. Psaltis, Appl. Phys. Lett. **94**, 161110 (2009).
[14]M. I. Lapsley, I. K. Chiang, Y. B. Zheng, X. Ding, X. Mao, and T. J. Huang, Lab Chip **11**, 1795 (2011).
[15]P. Domachuk, C. Grillet, V. Ta'eed, E. Mägi, J. Bolger, B. J. Eggleton, L. E. Rodd, and J. Cooper-White, Appl. Phys. Lett. **86**, 024103 (2005).
[16]L. K. Chin, A. Q. Liu, J. B. Zhang, C. S. Lim, and Y. C. Soh, Appl. Phys. Lett. **93**, 164107 (2008).
[17]P. Y. Chiou, Aaron T. Ohta, and Ming C. Wu, Nature **436**, 370 (2005).
[18]Y. Fainman, L. P. Lee, D. Psaltis, and C. Yang, *Optofluidics: Fundamentals, Devices, and Applications* (McGraw-Hill, New York, 2009).
[19]K. Campbell, A. Groisman, U. Levy, L. Pang, S. Mookherjea, D. Psaltis, and Y. Fainman, Appl. Phys. Lett. **85**, 6119 (2004).
[20]D. B. Wolfe, R. S. Conroy, P. Garstecki, B. T. Mayers, M. A. Fischbach, K. E. Paul, M. Prentiss, and G. M. Whitesides, Proc. Natl. Acad. Sci. U.S.A. **101**, 12434 (2004).
[21]A. Groisman, S. Zamek, K. Campbell, L. Pang, U. Levy, and Y. Fainman, Opt. Express **16**, 13499 (2008).
[22]Y. C. Seow, S. P. Lim, and H. P. Lee, Appl. Phys. Lett. **95**, 114105 (2009).
[23]W. Song and D. Psaltis, Lab Chip **11**, 2397 (2011).
[24]J. M. Lim, J. P. Urbanski, T. Thorsen, and S. M. Yang, Appl. Phys. Lett. **98**, 044101(2011).
[25]M. I. Lapsley, S.-C. S. Lin, X. Mao, and T. J. Huang, Appl. Phys. Lett. **95**, 083507 (2009).
[26]X. Mao, B. K. Juluri, M. I. Lapsley, Z. S. Stratton, and T. J. Huang, Microfluid. Nanofluid. **8**, 139 (2010).
[27]D. Ahmed, X. Mao, B. K. Juluri, and T. J. Huang, Microfluid. Nanofluid. **7**, 727 (2009).
[28]D. Ahmed, X. Mao, J. Shi, B. K. Juluri, and T. J. Huang, Lab Chip **9**, 2738 (2009).
[29]B. G. Dambrine and J.-B. Salmon, New J. Phys. **11**, 75015 (2009).
[30]F. Jiang, K. S. Drese, S. Hardt, M. Küpper, and F. Schönfeld, AIChE J. **50**, 2297 (2004).